CLDN15 is a novel diagnostic marker for malignant pleural mesothelioma

学　位　論　文

CLDN15 is a novel diagnostic marker for malignant pleural mesothelioma

（CLDN15 の悪性胸膜中皮腫新規診断マーカーとしての有用性）

福島県立医科大学大学院医学研究科

腫瘍専門医養成コース　呼吸器外科学講座

渡部　晶之

CLDN15 is a novel diagnostic marker for malignant pleural mesothelioma

Masayuki Watanabe
Department of Chest Surgery and Department of Basic Pathology, Graduate School of Medicine, Fukushima Medical University, Fukushima, Japan.

Abstract

Malignant mesothelioma is a cancer with a poor survival rate. It is difficult to diagnose mesotheliomas because they show a variety of histological patterns similar to those of various other cancers. However, since currently used positive markers for mesotheliomas may show false positives or false negatives, a novel mesothelial positive marker is required. In the present study, we screened 25 claudins and found that claudin-15 is expressed in the mesothelial cells. We made new rat anti-human claudin-15 (CLDN15) monoclonal antibodies that selectively recognize CLDN15, and investigated whether CLDN15 is a good positive marker for malignant pleural mesotheliomas (MPMs) using MPM tissue samples by immunohistochemistry and semi-quantification of the expression level using an immunoreactive score (IRS) method. Of 42 MPM samples, 83% were positive for CLDN15. The positive ratio was equal to or greater than other positive markers for MPMs including calretinin (81%), WT-1 (50%), and D2-40 (81%). In 50 lung adenocarcinoma sections, four cases were positive for CLDN15 and the specificity (92%) was comparable with other markers (90-100%). Notably, CLDN15 was rarely detected in 24 non-mesothelial tumors in the tissue microarray (12/327 cases). In conclusion, CLDN15 can be used in the clinical setting as a positive marker for MPM diagnosis.

Introduction

Malignant mesothelioma is a cancer with a poor survival rate[1,2] . It originates from mesothelial cells that cover the outer layer of serous membranes, including the pleura, peritoneum, pericardium, and tunica vaginalis testis. Malignant pleural mesotheliomas (MPMs) account for 85.5% of the total malignant mesotheliomas[3]. Histologically, MPMs are divided into epithelioid, biphasic and sarcomatoid subtypes. MPMs are principally caused by exposure to asbestos, and it typically takes 30–40 years to develop a tumor after initial asbestos exposure[2-4]; however, its pathogenesis has yet been established[5]. In the majority of developed countries, asbestos production, handling and use are limited and asbestos consumption has fallen to negligible levels. However, dismantling of buildings containing asbestos is expected to increase in future, and asbestos use is unfortunately still not prohibited in some developing countries. Therefore, malignant mesothelioma will continue to represent a significant global health concern.

Symptoms of MPM include breathlessness, chest pain, fatigue, anorexia, and weight loss[6], which are similar to those of lung adenocarcinoma. However, the treatment and prognosis are completely different. Treatment of MPMs mainly includes surgery, chemotherapy, and radiotherapy. Even if MPM patients receive these treatments, the median survival is limited to 9-12 months[7]. On the other hand, the survival rate of lung adenocarcinoma has been improving due to the development of targeted therapies and immunotherapeutic agents[8].

It is difficult to diagnose mesotheliomas because they show various

histological patterns similar to those of other cancers. In particular, it is important to distinguish MPMs from lung adenocarcinomas. The histology of epithelioid-type mesothelioma is often solid, tubulopapillary, and trabecular, which resembles that of lung adenocarcinomas. To discriminate MPMs from other tumors, immunohistochemical staining is required to confirm that at least two markers of mesothelial lineage are positive and at least two markers of epithelial lineage are negative[9]. Calretinin, WT-1 (Wilms' tumor 1), D2-40 (Podoplanin), and CK (Cytokeratin) 5/6 are clinically used as positive markers for epithelioid-type MPMs and carcinoembryonic antigen (CEA), claudin-4, thyroid transcription factor (TTF)-1, Napsin A, MOC31 and BerEP4 are used as negative markers. Although the sensitivities of Calretinin (nearly 100%), D2-40 (80-100%), and CK5/6 (75-100%) are high in the epithelioid-type MPMs, they are not exclusively specific to MPMs[10,11]. Calretinin and D2-40 are focally positive in 5-10% and about 15% of lung adenocarcinomas, respectively, and CK5/6 is positive in almost 100% of squamous carcinomas[10]. On the other hand, WT-1 has very high specificity, but its sensitivity is about 70-95% in the epithelioid-type MPMs[10]. In the sarcomatoid-type MPMs (and the sarcomatoid part of the biphasic MPMs), the sensitivity of these mesothelial markers are lower: Calretinin (50-60%), WT-1 (10-45%), D2-40 (75-90%), and CK5/6 (13-29%)[11]. Therefore, additional mesothelial positive markers with high sensitivity and specificity have been explored[12,13].

Claudins (CLDNs) are major components of tight junctions, which seal the intercellular spaces between adjacent cells, such as epithelial and endothelial cells. They are four-transmembrane proteins with typically ~22-kDa

molecular weight. The CLDN family comprises more than 24 members in human and mice, and specific combinations of CLDNs are expressed in normal epithelial tissues. In addition, CLDNs exhibit aberrant expression in a variety of cancer tissues[14-16], some of which are used as diagnostic and/or prognostic markers for the cancer[17-19]. To date, only a few reports on the expression profile of CLDNs in mesothelial tissues exist[20]. It is also unknown which CLDN proteins are expressed in human malignant mesothelioma tissues. On the other hand, several lines of evidence indicate that the expression of *CLDN15* mRNA is overexpressed in the epithelioid subtype of MPMs[21-24], which accounts for approximately 60% of MPM cases[25].

Here, we investigated the expression and localization of CLDNs in normal mesothelial tissues and found that CLDN15 was the most abundantly expressed claudin in these tissues. Using a novel CLDN15-targeting monoclonal antibody (mAbs), we examined the expression of CLDN15 in human MPM tissue specimens and propose that CLDN15 can be a good positive marker for MPMs.

Results

Expression of claudin-15 in normal mesothelium in mice

To identify claudin(s) expressed in mesothelial cells, we conducted a comprehensive RT-PCR screening using mouse pleura and peritoneum and specific primer sets for all claudins (Fig. 1a). Among the 24 claudin members, only Cldn1, Cldn3, Cldn10b, Cldn12, and Cldn15 were detected in pleura tissue. In peritoneum tissue, Cldn5 was also detected, which is probably caused by a contamination of mesentery blood vessels. To directly compare the expression levels of these five claudin subtypes, we conducted real-time PCR using DNA fragments with titrated concentrations as standards, and calculated the expression levels of each claudin (Fig. 1b). As a result, Cldn15 was most abundantly expressed in both the pleura and peritoneum tissues. To confirm that Cldn15 is expressed in mesothelial cells, we immunostained mouse pleura, peritoneum, pericardium, and tunica vaginalis (Fig. 1c). In all mesothelial tissues examined, Cldn15 was detected at the cell-cell junctions of the mesothelial cells, which is consistent with the fact that claudin is a component of tight junctions. These data indicate that Cldn15 is the major claudin expressed in mesothelial cells in mice.

Establishment of novel rat anti-human CLDN15 antibodies

To examine the expression of CLDN15 in human specimens, we newly generated mAbs that are highly specific for CLDN15. Since the claudin proteins have high amino-acid sequence homology among family members, some antibodies against a claudin cross-react with other claudin members. We chose

an immunogen peptide specific to CLDN15 in order to avoid any cross-reaction with other claudin members (Fig. 2a). We decided on amino-acid sequences of the cytoplasmic tails of human CLDN15 without homology with five representative claudins (Fig. 2b). We immunized rats with the peptide and screened for hybridomas producing an antibody applicable for immunohistochemistry (IHC). We then isolated an antibody clone (2C11), which specifically recognizes CLDN15 by IHC of formalin-fixed paraffin-embedded (FFPE) samples of CLDN15-overexpressing HEK293T cells (Fig. 2c). We also detected endogenous CLDN15 using 2C11 by IHC of an FFPE sample of human colon adenocarcinoma cell line Caco-2 cells (see Supplemenatry Fig. S1 online). To determine the epitope of this antibody, we generated 20 mutants of CLDN15 in which four amino acids in the immunogen region are replaced with alanine or threonine (Fig. 2b). Using HEK293T cell lysates expressing these mutants, we identified amino acids 219–226 (FGKYGRNA) as the epitope of 2C11 (Fig. 2d). We also isolated another CLDN15-specific clone, 3H11, which recognizes the region of amino acids 216–223 (DSSFGKYG) (see Supplementary Fig. S2 online). Furthermore, we determined the amino-acid sequences of the complementary determining region (CDR) of the 2C11 and 3H11 antibodies (Fig. 2e and Supplementary Fig. S2c online).

CLDN15 protein is expressed in MPM tissues

Next, we examined FFPE samples of MPMs using the newly established anti-CLDN15 antibody 2C11. We collected tissue samples of 42 cases diagnosed

as MPM. The background of the patients, including age, gender, histological type, asbestos exposure, stage (UICC, 8th[26]), and overall survival, is shown in Table 1. We examined the expression of CLDN15 in MPM tissue samples by immunohistochemistry using the 2C11 clone, and found that the membrane, as well as the cytoplasm, of only the tumor cells are positive for CLDN15 (Fig. 3, a and b). We semi-quantified the expression levels of CLDN15 using an immunoreactive score (IRS) method. We classified the staining intensity (I) of the CLDN15 signal into four categories (Fig. 3a), and the proportion (P) of the staining-positive areas into five categories, and calculated the IRS (I × P) (for details, see the Materials and Methods). Cells with either membranous or cytoplasmic stain were considered as CLDN15-positive. When the cut-off value of the IRS was set to 3, 83% of the MPM samples were positive for CLDN15 (Fig. 3d, Table 2). A similar staining pattern was obtained using another anti-CLDN15 clone, 3H11 (see Supplementary Fig. S2 online). The positive ratio was equal to or greater than the other positive diagnostic markers for MPMs, calretinin (81%), WT-1 (50%), and D2-40 (81%). The positive ratio of CLDN15 was significantly higher than that of WT-1 ($p = 0.0057$). The positive ratio was different in each histological type. In the epithelioid type, the positive ratio for CLDN15 was 93%, which was similar to or even greater than the other markers (Calretinin, 93%; WT-1, 50%; D2-40, 86%). Again, the difference between CLDN15 and WT-1 was significant ($p = 0.0022$). In the biphasic type, CLDN15 was positive in 75%, which was similar to the other markers (Calretinin, 75%; WT-1, 63%; D2-40, 75%). The intensity and proportion in the epithelioid-type cell region was higher than those in the sarcomatoid-type cell region (Fig. 3b).

In the sarcomatoid type, CLDN15 was positive in 50% of cases, which is comparable with the other markers (Calretinin, 33%; WT-1, 33%; D2-40, 67%) (Table 2). There was no significant difference in the sensitivity between any two markers in the biphasic and sarcomatoid types, although we could not rule out the possibility that there is a difference in the sensitivity among these markers since the statistical power was relatively low (0.20-0.28) due to small case numbers in these MPM types. In comparison to epithelioid-type MPMs, CLDN15 was significantly less positive in biphasic/sarcomatoid-type MPMs ($p = 0.028$).

Since diagnostic markers are often applied in combination in clinical practice, we examined the sensitivity of two-marker panels (Table 2). Combination of two markers increased the sensitivity. For example, 93% of the samples were positive for CLDN15 or Calretinin (Table 2, middle). There were no statistically significant differences in the sensitivity between any two-marker panels, which is probably due to small sample size and low statistical power (0.20-0.35). 71% of samples were positive for both CLDN15 and Calretinin, indicating that the positivity of CLDN15 and Calretinin does not completely overlap (Table 2, bottom).

CLDN15 is rarely expressed in other cancers

Since it is clinically important to differentiate lung adenocarcinomas from MPMs, we immunostained lung adenocarcinoma sections for CLDN15 and other positive markers. In the present study, 4/50 (8%) cases were positive for CLDN15, and the specificity was comparable with other markers (Calretinin, 4/40 [10%]: WT-1, 1/40 [2%]; D2-40, 0/40 [0%]) (Fig. 3c-d, Table 2). In the two-

marker panels, the specificity was 83-98% and only one lung adenocarcinoma sample expressed two markers simultaneously. We also investigated the expression of CLDN15 on non-mesothelioma tumors by using tissue microarrays of 24 primary tumors. CLDN15 was expressed in only 12/327 (4%) cases (Fig. 3 e-h, Table 3).

Discussion

Although several reports suggested that the expression level of the *CLDN15* transcript is elevated in MPM tissues[22-24,27], to date there has been no report examining the protein expression of CLDN15 in MPMs. In this study, we showed that claudin-15 is the most abundantly expressed claudin in mesothelial tissues and demonstrated that CLDN15 protein is also detected at a high level in MPM tissues using newly established anti-human CLDN15 mAbs. Furthermore, CLDN15 was negative in most tumors examined, including lung adenocarcinomas. Thus, we propose that CLDN15 is a promising positive marker for MPMs in clinical applications.

IHC is the most useful and standard method for the diagnosis of MPMs. The most required property as a positive marker is its high sensitivity. In this respect, the positive rate of CLDN15 in MPMs was 83%, which is equivalent to the conventional typical positive markers, such as Calretinin (81%), WT-1 (50%), and D2-40 (81%). Although Calretinin is widely used as a positive marker for MPMs, the proportion of the staining-positive area for Calretinin is not always high[10]. On the other hand, CLDN15 is often positive over a large portion of cancerous tissue, which is beneficial for the diagnosis of small samples, such as biopsy tissues. The positive rate of CLDN15 was as high as 93% in the epithelioid-type MPMs, while the sensitivity of CLDN15 in sarcomatoid-type MPMs was not so high (50%). This may reflect the reduced expression of CLDN15 in the less differentiated (more advanced) sarcomatoid types. Since the positivity for CLDN15 and Calretinin does not completely

match, some cases are CLDN15-positive and Calretinin-negative, and vice versa. This indicates that the combinational application of CLDN15 and Calretinin (and other markers) can achieve much higher sensitivity (93% in our samples).

In addition to sensitivity, the immunohistochemical markers should have high specificity to distinguish MPMs from other types of cancers. An important cancer to differentiate from MPM is lung adenocarcinoma; the false-positive rate of CLDN15 in lung adenocarcinoma was 8%, which is comparable with other MPM-positive markers, such as calretinin (10%). In lung squamous cell carcinomas, which are another cancer to be distinguished from MPMs, we found no false positives for CLDN15 (n = 11). Since cancers of other organs may metastasize to the pleura, we also immunostained non-mesothelioma tumors other than lung cancers. CLDN15 was positive in only 12 out of 327 cases. Positive predictive value (PPV) and negative predictive value (NPV) are also important when using antibodies clinically. In this study, the PPV and NPV were 90% and 87%, respectively. However, since the frequency of MPMs is significantly lower than that of lung adenocarcinomas, the PPV is considered to be even lower. Furthermore, as the number of cases examined in this study was not large, the result should be further validated in larger cohorts. Currently, we concluded that CLDN15 has a high specificity comparable to current positive markers in clinical use.

The differential diagnosis of MPMs has been challenging because of the histological variety and morphological similarities with other cancers. Current diagnosis relies on immunostaining using a combination of multiple positive and

negative markers, which have varied specificity and sensitivity. Since an increasing number of MPM cases is predicted in the upcoming decades, the establishment of a novel strategy using a differential combination of diagnostic markers is anticipated.

Although the anti-CLDN15 antibodies we established have high sensitivity and specificity (Fig. 3, Table 2 and 3), the CLDN15 signal was at the cytoplasm as well as membranes, which is in contrast to the exclusive membrane staining patterns of many other anti-CLDN antibodies. This may be due to internalization of CLDN15 into the cytoplasm when overexpressed. Indeed, overexpressed CLDN15 is localized at the cytoplasm in HEK293T cells (Fig. 2c). A similar change in claudin localization has been reported for CLDN1 in breast cancer, colon cancer and tongue carcinoma; the localization of CLDN1 changes from the membrane to the cytoplasm as the malignancy progresses[28,29]. Claudin is thought to be less susceptible to protease action, and no degradation products have been reported so far. Therefore, it is considered difficult to use it as a diagnostic marker in the pleural effusion or blood. However, since CLDN15 is expected to be expressed in the MPM cells in the pleural effusion, it may be useful for diagnosis to examine the immunostaining of the pleural effusion cell blocks.

As for treatment strategies, there are only few effective treatments for unresectable MPMs. Platinum-based chemotherapy is the current first-line standard therapy for unresectable MPMs[30-32]. There was no recommended therapy for MPMs that have progressed after first-line chemotherapy. Thus, the development of new therapeutic strategies has been ongoing for long time. In

recent years, several clinical trials have shown the effectiveness of immune checkpoint inhibitors such as the anti-programmed cell death 1 (PD-1) antibody against MPMs[33-35]. Therefore, it has become the standard therapy to administer anti-PD-1 antibody for patients with relapsed MPM who have received platinum-based chemotherapy[36]. In the future, it may be possible to predict the effects of immune checkpoint inhibitors if the expression levels of CLDN15 and PD-L1 are correlated. In addition, various gene mutations were recently identified in MPMs, but molecular-targeted therapeutic agents such as those for non-small cell lung cancer have not yet been developed[37].

The results of this study suggest that CLDN15 is a therapeutic target for MPMs. Since CLDN15 is expressed on the cell surfaces of MPM cells specifically, it would be a potential target for anti-cancer drugs. There may be several strategies for developing a new treatment of MPMs targeting CLDN15, one of which is developing antibodies against the extracellular region of CLDN15 with antibody-dependent cellular cytotoxicity[38]. Another strategy is an antibody-drug conjugate[39]. Radioimmunotherapy using radiolabeled antibody is also considerable because MPMs are regarded as radiosensitive[40-42]. In addition, chimeric antigen receptor (CAR)-T cell therapy is also attractive. CAR-T approach targeting the extracellular domain of another claudin (CLDN6) has been shown to successfully mediate a complete regression of CLDN6-expressing human tumor cells xenografted in immunodeficient mice[43]. However, it should be noted that CLDN15 constitutes the tight junctions of the normal intestinal epithelial cells and renal endothelial cells[44,45], which might bear the risk of off-target toxicity in these approaches.

Because MPMs are rare tumors compared with lung cancers, it is difficult to find a large number of patients to enroll. Therefore, future studies with larger cohorts would further validate the results of the current study.

In conclusion, we revealed that IHC of CLDN15 has high sensitivity and specificity for MPM tissues in human. The results strongly support the potency of CLDN15 as a positive marker for the pathological diagnosis of MPM in clinical application.

Methods

Ethics approval and consent to participate

This study was reviewed by the Ethics Committee of Fukushima Medical University, approved by the president of the university (approval number 2512). The requirement for patients' informed consent was waived and the patients were given the right to opt-out from the research, which was stated on the website of Fukushima Medical University. This study was carried out in accordance with the Declaration of Helsinki and in compliance with the Japanese Ethical Guidelines for Medical and Health Research involving Human Subjects.

Animal experiments

The experiments conducted using animals strictly adhered to the compliance standards of the Japanese Guidelines for Proper Conduct of Animals Experiments and ARRIVE guidelines. The protocols of the animal experiments (approval numbers 29098, 2019023, and 30112) were reviewed by the Fukushima Medical University Animal Care and Use Committee, and were approved by the president of the university.

Patients and histological samples

The tissues were obtained from patients who were diagnosed as having malignant mesothelioma or lung adenocarcinoma between 2003 and 2019 at Fukushima Medical University Hospital and its partner hospitals. The multi organ tumor tissue array slide (MC6163) was purchased from US Biomax Inc

(Derwood, MD, USA).

Immunohistochemical staining of formalin-fixed paraffin-embedded samples

All the tissues of malignant pleural mesothelioma and lung adenocarcinoma were fixed with 10% formalin, embedded in paraffin, and subjected to Hematoxylin-Eosin (HE) staining or immunohistochemical staining. The sections of the samples were deparaffinized with 100% xylene and washed with 100% ethanol. The sections were then treated with 0.3% hydrogen peroxide-containing methanol at room temperature (RT) for 20 minutes to inactivate the endogenous peroxidase followed by 0.1% semicarbazide hydrochloride (#192-00372; Fujifilm-WAKO, Osaka, Japan) in distilled water for 1 h at RT and Immunosaver (Nissin EM, Tokyo Japan) at 70ºC for 16 h. Blocking was performed with 5% non-fat dry milk (#0646869; Morinaga Milk Industry) in phosphate-buffered saline (PBS). The sections were treated with primary antibody in PBS containing 2% bovine serum albumin (BSA) at 4ºC overnight. The secondary antibody reaction was carried out at RT for 30 min. Then, the sections were developed with 3,3'-Diaminobenzidine (DAB) solution (50 mM Tris buffer [pH. 7.5], 0.02% [w/w] DAB, 30%, 0.005% hydrogen peroxide) for 20 min at RT, and counter-stained with hematoxylin. Samples were dehydrated with 100% ethanol and then 100% xylene, and embedded. The samples were observed using an optical phase contrast microscope (OLYMPUS BX61, OLYMPUS, Tokyo, Japan), and images were taken with a DP controller (OLYMPUS).

Histological evaluation

After masking the patient background, two pathologists and one thoracic surgeon semi-quantified the CLDN15 protein expression using an immunoreactive score (IRS; partially modified from Remmele W et al.[46]) method. We classified the staining intensity (I) of the CLDN15 signal into four categories (0 [negative], 1 [weak], 2 [moderate], and 3 [strong]) and the proportion (P) of staining-positive areas in the tumor into five categories (0 [<1%], 1 [1–10%], 2 [11–30], 3 [31–50%], and 4 [50%<]). Then, “I” and “P” were multiplied to obtain IRS (IRS = I × P).

Statistical analysis

Statistical significance of differences was evaluated by the Fisher's Exact test with Bonferroni's correction. The p-value was calculated by Excel software and $p < 0.05$ was considered to be statistically significant. The statistical power was calculated by G*Power software using the phi (ϕ) coefficient as the effect size.

Acknowledgements

We greatly appreciate Yukiko Kikuta, Eiko Otomo, Kayoko Kobayashi, Eriko Hoshi, Abidur Rahman, Ayumi Hozumi and Keiko Watari for their technical assistance, as well as Dr. Yoshihiro Nozawa and Dr. Yuko Hashimoto for their management of the clinical samples. We would also like to express our gratitude to the Scientific English Editing Section of Fukushima Medical University, for their proofreading of our manuscript. This work was supported by JSPS KAKENHI Grant Number JP19K18224 to M.W.

Author contributions

Conceptualization: T.H. and H.C. Methodology: T.H. Formal analysis, M.W., K.S. and H.C. Investigation: M.W., T.H., K.O and A.H. Resources: T.H., A.H., H.M., H.T., Y.O., S.M., N.O., Y.M., T.Ha. and Y.S. Data curation: M.W. Writing - original draft: M.W. Writing - review & editing: T.H., H.M, H.T., Y.O., S.M., N.O., Y.M., T.Ha., T.S., H.S. and H.C. Visualization: M.W. and T.H. Supervision: H.S. and H.C. Project administration: T.H. Funding acquisition: M.W.

Competing interests

The authors declare no competing interest.

Availability of materials and data

The datasets and monoclonal antibodies used in the current study are available from the corresponding author on reasonable request.

References

1 Bianchi, C. & Bianchi, T. Malignant mesothelioma: global incidence and relationship with asbestos. *Ind Health* **45**, 379-387, doi:10.2486/indhealth.45.379 (2007).

2 Robinson, B. W. S. & Lake, R. A. Advances in Malignant Mesothelioma. *N Engl J Med* **353**, 1591-1603, doi:10.1056/nejmra050152 (2005).

3 Gemba, K. *et al.* National survey of malignant mesothelioma and asbestos exposure in Japan. *Cancer Sci* **103**, 483-490, doi:10.1111/j.1349-7006.2011.02165.x (2012).

4 Wagner, J. C., Sleggs, C. A. & Marchand, P. Diffuse pleural mesothelioma and asbestos exposure in the North Western Cape Province. *Br J Ind Med* **17**, 260-271, doi:10.1136/oem.17.4.260 (1960).

5 Yap, T. A., Aerts, J. G., Popat, S. & Fennell, D. A. Novel insights into mesothelioma biology and implications for therapy. *Nat Rev Cancer* **17**, 475-488, doi:10.1038/nrc.2017.42 (2017).

6 Clayson, H., Seymour, J. & Noble, B. Mesothelioma from the patient's perspective. *Hematol Oncol Clin North Am* **19**, 1175-1190, viii, doi:10.1016/j.hoc.2005.09.003 (2005).

7 Taioli, E. *et al.* Determinants of Survival in Malignant Pleural Mesothelioma: A Surveillance, Epidemiology, and End Results (SEER) Study of 14,228 Patients. *PLoS ONE* **10**, e0145039, doi:10.1371/journal.pone.0145039 (2015).

8 Myers, D. J. & Wallen, J. M. Lung Adenocarcinoma. *StatPearls* (StatPearls Publishing Copyright © 2021, StatPearls Publishing LLC., 2021).

9 Travis, W. D., Brambilla, E., Burke, A. P., Marx, A. & Nicholson, A. G. Introduction to The 2015 World Health Organization Classification of Tumors of the Lung, Pleura, Thymus, and Heart. *J Thorac Oncol* **10**, 1240-1242, doi:10.1097/jto.0000000000000663 (2015).

10 Husain, A. N. *et al.* Guidelines for Pathologic Diagnosis of Malignant Mesothelioma 2017 Update of the Consensus Statement From the International Mesothelioma Interest Group. *Arch Pathol Lab Med* **142**, 89-108, doi:10.5858/arpa.2017-0124-ra (2018).

11 Chapel, D. B., Schulte, J. J., Husain, A. N. & Krausz, T. Application of immunohistochemistry in diagnosis and management of malignant mesothelioma. *Translational Lung Cancer Research* **9**, S3-S27,

doi:10.21037/tlcr.2019.11.29 (2020).

12 Washimi, K. *et al.* Specific expression of human intelectin-1 in malignant pleural mesothelioma and gastrointestinal goblet cells. *PLoS ONE* **7**, e39889, doi:10.1371/journal.pone.0039889 (2012).

13 Tsuji, S. *et al.* HEG1 is a novel mucin-like membrane protein that serves as a diagnostic and therapeutic target for malignant mesothelioma. *Sci Rep* **7**, 45768, doi:10.1038/srep45768 (2017).

14 Oliveira, S. S. & Morgado-Díaz, J. A. Claudins: multifunctional players in epithelial tight junctions and their role in cancer. *Cell Mol Life Sci* **64**, 17-28, doi:10.1007/s00018-006-6314-1 (2007).

15 Osanai, M., Takasawa, A., Murata, M. & Sawada, N. Claudins in cancer: bench to bedside. *Pflugers Arch* **469**, 55-67, doi:10.1007/s00424-016-1877-7 (2017).

16 Tabaries, S. & Siegel, P. M. The role of claudins in cancer metastasis. *Oncogene* **36**, 1176-1190, doi:10.1038/onc.2016.289 (2017).

17 Lanigan, F. *et al.* Increased claudin-4 expression is associated with poor prognosis and high tumour grade in breast cancer. *Int J Cancer* **124**, 2088-2097, doi:10.1002/ijc.24159 (2009).

18 Ouban, A. Claudin-1 role in colon cancer: An update and a review. *Histol Histopathol* **33**, 1013-1019, doi:10.14670/hh-11-980 (2018).

19 Singh, A. B. & Dhawan, P. Claudins and cancer: Fall of the soldiers entrusted to protect the gate and keep the barrier intact. *Semin Cell Dev Biol* **42**, 58-65, doi:10.1016/j.semcdb.2015.05.001 (2015).

20 Markov, A. G. *et al.* Tight junction proteins contribute to barrier properties in human pleura. *Respir Physiol Neurobiol* **175**, 331-335, doi:10.1016/j.resp.2010.12.012 (2011).

21 Blum, Y. *et al.* Dissecting heterogeneity in malignant pleural mesothelioma through histo-molecular gradients for clinical applications. *Nat Commun* **10**, 1333, doi:10.1038/s41467-019-09307-6 (2019).

22 Bueno, R. *et al.* Comprehensive genomic analysis of malignant pleural mesothelioma identifies recurrent mutations, gene fusions and splicing alterations. *Nat Genet* **48**, 407-416, doi:10.1038/ng.3520 (2016).

23 Gordon, G. J. *et al.* Identification of Novel Candidate Oncogenes and Tumor Suppressors in Malignant Pleural Mesothelioma Using Large-Scale Transcriptional Profiling. *Am J Pathol* **166**, 1827-1840, doi:10.1016/s0002-9440(10)62492-3 (2005).

24 Rouka, E. *et al.* Transcriptomic Analysis of the Claudin Interactome in Malignant Pleural Mesothelioma: Evaluation of the Effect of Disease Phenotype, Asbestos Exposure, and CDKN2A Deletion Status. *Front Physiol* **8**, 156, doi:10.3389/fphys.2017.00156 (2017).

25 Inai, K. Pathology of mesothelioma. *Environ Health Prev Med* **13**, 60-64, doi:10.1007/s12199-007-0017-6 (2008).

26 Berzenji, L., Van Schil, P. E. & Carp, L. The eighth TNM classification for malignant pleural mesothelioma. *Transl Lung Cancer Res* **7**, 543-549, doi:10.21037/tlcr.2018.07.05 (2018).

27 Kanamori-Katayama, M. *et al.* LRRN4 and UPK3B Are Markers of Primary Mesothelial Cells. *PLoS ONE* **6**, e25391, doi:10.1371/journal.pone.0025391 (2011).

28 Bhat, A. A. *et al.* Claudin-1, A Double-Edged Sword in Cancer. *Int J Mol Sci* **21**, 569, doi:10.3390/ijms21020569 (2020).

29 Yamamoto, D. *et al.* Intracellular claudin-1 at the invasive front of tongue squamous cell carcinoma is associated with lymph node metastasis. *Cancer Sci* **111**, 700-712, doi:10.1111/cas.14249 (2020).

30 Vogelzang, N. J. *et al.* Phase III study of pemetrexed in combination with cisplatin versus cisplatin alone in patients with malignant pleural mesothelioma. *J Clin Oncol* **21**, 2636-2644, doi:10.1200/jco.2003.11.136 (2003).

31 Ceresoli, G. L. *et al.* Phase II study of pemetrexed plus carboplatin in malignant pleural mesothelioma. *J Clin Oncol* **24**, 1443-1448, doi:10.1200/jco.2005.04.3190 (2006).

32 Castagneto, B. *et al.* Phase II study of pemetrexed in combination with carboplatin in patients with malignant pleural mesothelioma (MPM). *Ann Oncol* **19**, 370-373, doi:10.1093/annonc/mdm501 (2008).

33 Okada, M. *et al.* Clinical Efficacy and Safety of Nivolumab: Results of a Multicenter, Open-label, Single-arm, Japanese Phase II study in Malignant Pleural Mesothelioma (MERIT). *Clin Cancer Res* **25**, 5485-5492, doi:10.1158/1078-0432.Ccr-19-0103 (2019).

34 Quispel-Janssen, J. *et al.* Programmed Death 1 Blockade With Nivolumab in Patients With Recurrent Malignant Pleural Mesothelioma. *J Thorac Oncol* **13**, 1569-1576, doi:10.1016/j.jtho.2018.05.038 (2018).

35 Scherpereel, A. *et al.* Nivolumab or nivolumab plus ipilimumab in patients with relapsed malignant pleural mesothelioma (IFCT-1501 MAPS2): a

multicentre, open-label, randomised, non-comparative, phase 2 trial. *Lancet Oncol* **20**, 239-253, doi:10.1016/s1470-2045(18)30765-4 (2019).

36 Ettinger, D. S. *NCCN Clinical Practice Guidelines in Malignant Pleural Mesothelioma*, https://www2.tri-kobe.org/nccn/guideline/lung/english/mpm.pdf (2019).

37 Yoshikawa, Y., Kuribayashi, K., Minami, T., Ohmuraya, M. & Kijima, T. Epigenetic Alterations and Biomarkers for Immune Checkpoint Inhibitors-Current Standards and Future Perspectives in Malignant Pleural Mesothelioma Treatment. *Front Oncol* **10**, 554570, doi:10.3389/fonc.2020.554570 (2020).

38 Nimmerjahn, F. & Ravetch, J. V. Fcgamma receptors as regulators of immune responses. *Nat Rev Immunol* **8**, 34-47, doi:10.1038/nri2206 (2008).

39 Hamilton, G. S. Antibody-drug conjugates for cancer therapy: The technological and regulatory challenges of developing drug-biologic hybrids. *Biologicals* **43**, 318-332, doi:10.1016/j.biologicals.2015.05.006 (2015).

40 Witzig, T. E. *et al.* Treatment with ibritumomab tiuxetan radioimmunotherapy in patients with rituximab-refractory follicular non-Hodgkin's lymphoma. *J Clin Oncol* **20**, 3262-3269, doi:10.1200/jco.2002.11.017 (2002).

41 Andersson, H. *et al.* Intraperitoneal alpha-particle radioimmunotherapy of ovarian cancer patients: pharmacokinetics and dosimetry of (211)At-MX35 F(ab')2--a phase I study. *J Nucl Med* **50**, 1153-1160, doi:10.2967/jnumed.109.062604 (2009).

42 Kratochwil, C. *et al.* 225Ac-PSMA-617 for PSMA-Targeted α-Radiation Therapy of Metastatic Castration-Resistant Prostate Cancer. *J Nucl Med* **57**, 1941-1944, doi:10.2967/jnumed.116.178673 (2016).

43 Reinhard, K. *et al.* An RNA vaccine drives expansion and efficacy of claudin-CAR-T cells against solid tumors. *Science* **367**, 446-453, doi:10.1126/science.aay5967 (2020).

44 Chiba, H., Osanai, M., Murata, M., Kojima, T. & Sawada, N. Transmembrane proteins of tight junctions. *Biochim Biophys Acta* **1778**, 588-600, doi:10.1016/j.bbamem.2007.08.017 (2008).

45 Kiuchi-Saishin, Y. *et al.* Differential expression patterns of claudins, tight junction membrane proteins, in mouse nephron segments. *J Am Soc*

Nephrol **13**, 875-886 (2002).

46 Remmele, W. *et al.* Comparative histological, histochemical, immunohistochemical and biochemical studies on oestrogen receptors, lectin receptors, and Barr bodies in human breast cancer. *Virchows Arch A Pathol Anat Histopathol* **409**, 127-147, doi:10.1007/bf00708323 (1986).

Figure legends

Figure 1. Claudin-15 is the major constituent of mesothelial tight junctions.

a. RT-PCR of mouse pleura and peritoneum using specific primers for claudins. Note that claudin-1, -5, -10b, -12 and -15 are expressed in the mesothelial tissues and that tight junction markers occludin and tricellulin were also detected. Genomic DNA and samples prepared without reverse transcriptase were used as positive and negative controls, respectively.

b. Real-time RT-PCR of claudins. The relative expression levels were calculated using purified DNA fragments of each claudin as a standard. Note that claudin-15 is most abundantly expressed in both the pleura and peritoneum samples.

c. Immunofluorescence staining of mesothelial tissues. Visceral and parietal pleura, visceral and parietal peritoneum, pericardium, and tunica vaginalis are stained for claudin-15 (green), HSPG (basement membrane marker, red) and DAPI (DNA, blue). Note that claudin-15 is localized at cell-cell junctions of mesothelial cells.

Figure 2. Establishment of a novel anti-CLDN15 mAb suitable for IHCs.

a. Schematic representation of the domain structure of human CLDN15 protein. The region corresponding to the peptide used for the immunization is shown in orange.

b. Amino-acid sequence of the cytoplasmic tail of CLDN15 and alanine mutants used in this study. Alignment with other CLDNs is also shown.

c. IHC of HEK293T cells expressing CLDNs. Note that 2C11 specifically stains only CLDN15-expressing cells.

d. Epitope analysis of 2C11. Note that 2C11 signal is lost in mutants 9–19, indicating that the epitope is ^{219}FGKYGRNA^{226} of CLDN15.

e. Amino-acid sequences of CDRs of 2C11.

Figure 3. CLDN15 is expressed in MPM tissues.

a. Typical staining patterns of anti-CLDN15 (2C11) mAb exhibiting strong to weak staining intensities. Scale bar, 50 μm.

b. IHC of epithelioid-, biphasic- and sarcomatoid-type MPMs using anti-CLDN15 (2C11), anti-calretinin, anti-D2-40 and anti-WT1 antibodies. "E" and "S" in the HE staining panel of the biphasic-type MPM indicate the epitheliod-type and sarcomatoid-type cell regions, respectively.

c. IHC of lung adenocarcinomas using anti-CLDN15 (2C11) mAb.

d. Distribution of IRS scores in MPMs and lung adenocarcinomas.

e. The ROC (receiver operator characteristic) curve shows that the cutoff value of 3 exhibits the best performance.

f-h. IHC of lung squamous cell carcinomas (f), chest wall fibrosarcoma (g) and abdominal wall fibrosarcoma (h) using anti-CLDN15 (2C11) mAb.

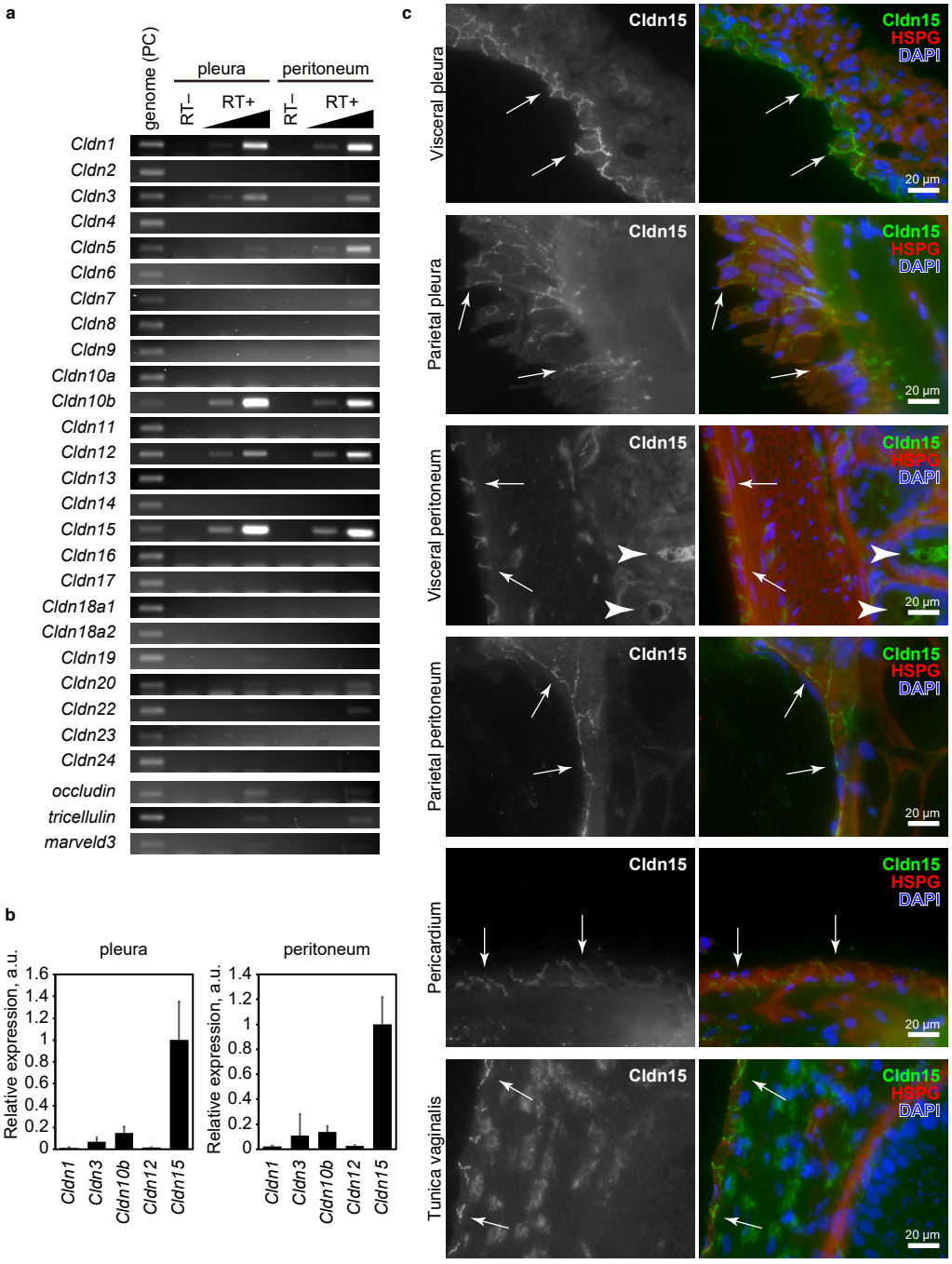
a
genome (PC)
pleura
peritoneum
RT–
RT+
RT–
RT+
Cldn1
Cldn2
Cldn3
Cldn4
Cldn5
Cldn6
Cldn7
Cldn8
Cldn9
Cldn10a
Cldn10b
Cldn11
Cldn12
Cldn13
Cldn14
Cldn15
Cldn16
Cldn17
Cldn18a1
Cldn18a2
Cldn19
Cldn20
Cldn22
Cldn23
Cldn24
occludin
tricellulin
marveld3
b
pleura
peritoneum
Relative expression, a.u.
Cldn1
Cldn3
Cldn10b
Cldn12
Cldn15
c
Visceral pleura
Parietal pleura
Visceral peritoneum
Parietal peritoneum
Pericardium
Tunica vaginalis
Cldn15
Cldn15
HSPG
DAPI
20 μm

Fig. 1

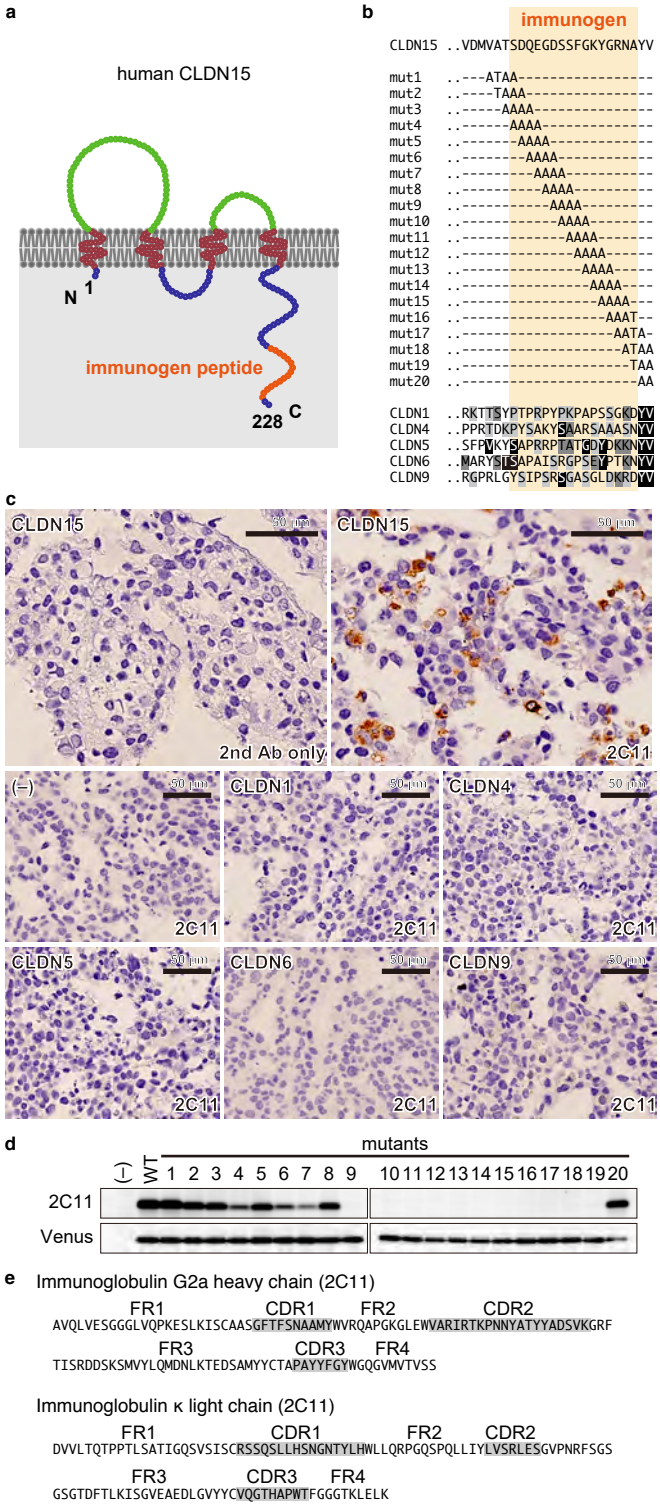
a
human CLDN15
N
1
immunogen peptide
228
C
b
immunogen
CLDN15 ..VDMVATSDQEGDSSFGKYGRNAYV
mut1 ..---ATAA----------
mut2 ..----TAAA----------
mut3 ..-----AAAA----------
mut4 ..------AAAA----------
mut5 ..-------AAAA----------
mut6 ..--------AAAA----------
mut7 ..---------AAAA----------
mut8 ..----------AAAA----------
mut9 ..-----------AAAA----------
mut10 ..------------AAAA--------
mut11 ..-------------AAAA-------
mut12 ..--------------AAAA------
mut13 ..---------------AAAA-----
mut14 ..----------------AAAA----
mut15 ..-----------------AAAA---
mut16 ..------------------AAAT--
mut17 ..-------------------AATA-
mut18 ..--------------------ATAA
mut19 ..---------------------TAA
mut20 ..----------------------AA
CLDN1 ..RKTTSYPTPRPYPKPAPSSGKDVV
CLDN4 ..PPRTDKPYSAKYSAARSAAASNVV
CLDN5 ..SFPVKYSAPRRPTATSDVDKKNVV
CLDN6 ..MARYSISAPAISRGPSEYPTKNVV
CLDN9 ..RGPRLGYSIPSRSGASGLDKRDVV
c
CLDN15
2nd Ab only
CLDN15
2C11
(–)
2C11
CLDN1
2C11
CLDN4
2C11
CLDN5
2C11
CLDN6
2C11
CLDN9
2C11
50 μm
d
mutants
(–)
WT
1 2 3 4 5 6 7 8 9 10 11 12 13 14 15 16 17 18 19 20
2C11
Venus
e
Immunoglobulin G2a heavy chain (2C11)
FR1 CDR1 FR2 CDR2
AVQLVESGGGLVQPKESLKISCAASGFTFSNAAMYWVRQAPGKGLEWVARIRTKPNNYATYYADSVKGRF
FR3 CDR3 FR4
TISRDDSKSMVYLQMDNLKTEDSAMYYCTAPAYYFGYWGQGVMVTVSS
Immunoglobulin κ light chain (2C11)
FR1 CDR1 FR2 CDR2
DVVLTQTPPTLSATIGQSVSISCRSSQSLLHSNGNTYLHWLLQRPGQSPQLLIYLVSRLESGVPNRFSGS
FR3 CDR3 FR4
GSGTDFTLKISGVEAEDLGVYYCVQGTHAPWTFGGGTKLELK

Fig. 2

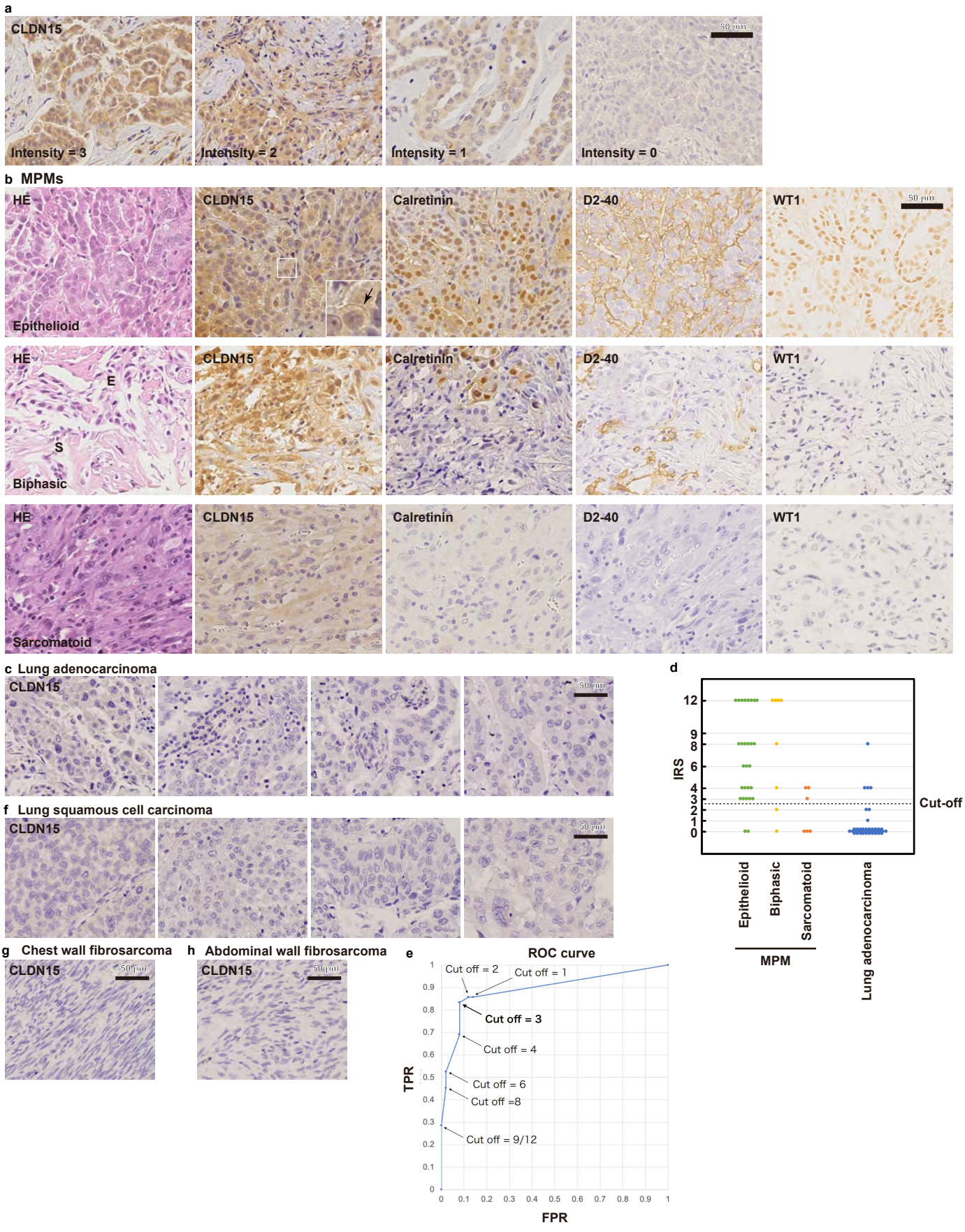
a
CLDN15
Intensity = 3
Intensity = 2
Intensity = 1
Intensity = 0
50 μm
b MPMs
HE
CLDN15
Calretinin
D2-40
WT1
Epithelioid
E
S
Biphasic
Sarcomatoid
c Lung adenocarcinoma
f Lung squamous cell carcinoma
g Chest wall fibrosarcoma
h Abdominal wall fibrosarcoma
d
IRS
Cut-off
Epithelioid
Biphasic
Sarcomatoid
Lung adenocarcinoma
MPM
e
ROC curve
TPR
FPR
Cut off = 2
Cut off = 1
Cut off = 3
Cut off = 4
Cut off = 6
Cut off =8
Cut off = 9/12

Fig. 3

Table 1. Clinicopathological features of MPM patients

Number of patients	N = 42
Age (years)	
Median	65.5
Range	21–86
Gender, n (%)	
Male	38 (90.5%)
Female	4 (9.5%)
Histological Type, n (%)	
Epithelioid	28 (66.7%)
Biphasic	8 (19.0%)
Sarcomatoid	6 (14.3%)
Asbestos exposure, n (%)	
Exposed	27 (64.3%)
Non-exposed	15 (35.7%)
Stage (UICC 8th)	
I	28 (66.7%)
II	2 (4.8%)
III	8 (19.0%)
IV	4 (9.5%)
Survival (months)	
Median	9
Range	2–64

Table 2. Expression of CLDN15 and other markers for MPM in three types of MPMs and lung adenocarcinoma tissues.

MPM type	CLDN15	Calretinin	WT-1	D2-40	Total
Epithelioid	26 (93%)**	26 (93%)**	14 (50%)	24 (86%)*	28
Biphasic	6 (75%)	6 (75%)	5 (63%)	6 (75%)	8
Sarcomatoid	3 (50%)	2 (33%)	2 (33%)	4 (67%)	6
Total	35 (83%)*	34 (81%)*	21 (50%)	34 (81%)*	42
Lung adenocarcinoma	4/50	4/40	1/40	0/40	
Specificity	92%	90%	98%	100%	

*, $p < 0.05$; **, $p < 0.005$ higher than the sensitivity of WT-1. Other pairs were not significantly different.

MPM type	CL15 or Cal	CL15 or WT1	CL15 or D2-40	Cal or WT1	Cal or D2-40	WT1 or D2-40
Epithelioid	28 (100%)	27 (96%)	28 (100%)	27 (96%)	27 (96%)	26 (93%)
Biphasic	7 (88%)	7 (88%)	7 (88%)	7 (88%)	8 (100%)	8 (100%)
Sarcomatoid	4 (67%)	4 (67%)	5 (83%)	3 (50%)	5 (83%)	5 (83%)
Total	39 (93%)	38 (90%)	40 (95%)	37 (88%)	40 (95%)	39 (93%)
Lung adenocarcinoma	7/40	5/40	4/40	5/40	4/40	1/40
Specificity	83%	88%	90%	88%	90%	98%

No pairs were significantly different.

MPM type	CL15 & Cal	CL15 & WT1	CL15 & D2-40	Cal & WT1	Cal & D2-40	WT1 & D2-40
Epithelioid	24 (71%)	13 (46%)†	22 (79%)	13 (46%)†	23 (82%)*	12 (43%)†
Biphasic	5 (63%)	4 (50%)	5 (63%)	4 (50%)	4 (50%)	3 (38%)
Sarcomatoid	1 (17%)	1 (17%)	2 (33%)	1 (17%)	1 (17%)	1 (17%)
Total	30 (71%)	18 (43%)	29 (69%)*	18 (43%)	28 (67%)	16 (38%)†
Lung adenocarcinoma	1/40	0/40	0/40	0/40	0/40	0/40
Specificity	98%	100%	100%	100%	100%	100%

†, $p<0.05$ lower than CL15&Cal; *, $p<0.05$ higher than WT1&D2-40. Other pairs were not significantly different.

Table 3. CLDN15 expression in the tissue microarray of non MPM primary tumors.

Organ	Malignant tumor	CLDN15	Specificity
Cerebrum	Astrocytoma	0/10	100%
	Glioblastoma	1/10	90%
Thyroid gland	Papillary carcinoma	0/10	100%
	Follicular cell carcinoma	1/10	90%
Lung	Squamous cell carcinoma	0/11	100%
	Large cell carcinoma	1/12	92%
	Small cell carcinoma	0/12	100%
Breast	Invasive ductal carcinoma	0/19	100%
Esophagus	Adenocarcinoma	0/10	100%
	Squamous cell carcinoma	0/10	100%
Stomach	Adenocarcinoma	0/20	100%
Liver	Hepatocellular carcinoma	1/17	94%
Pancreas	Duct adenocarcinoma	0/20	100%
Colon	Adenocarcinoma	0/11	100%
	Mucinous adenocarcinoma	0/7	100%
Kidney	Clear cell carcinoma	6/20	70%
Bladder	Invasive urothelial carcinoma	0/19	100%
Prostate	Adenocarcinoma	1/20	95%
Testis	Seminoma	0/10	100%
	Embryonal carcinoma	0/10	100%
Ovary	High grade serous carcinoma	1/9	89%
	Mucinous adenocarcinoma	0/10	100%
Cervix	Squamous cell carcinoma	0/20	100%
Uterus	Endometrioid adenocarcinoma	0/20	100%
	Total	12/327	96.3%

Supplementary information

CLDN15 is a novel diagnostic marker for malignant pleural mesothelioma

Masayuki Watanabe
Department of Chest Surgery and Department of Basic Pathology, Graduate School of Medicine, Fukushima Medical University, Fukushima, Japan.

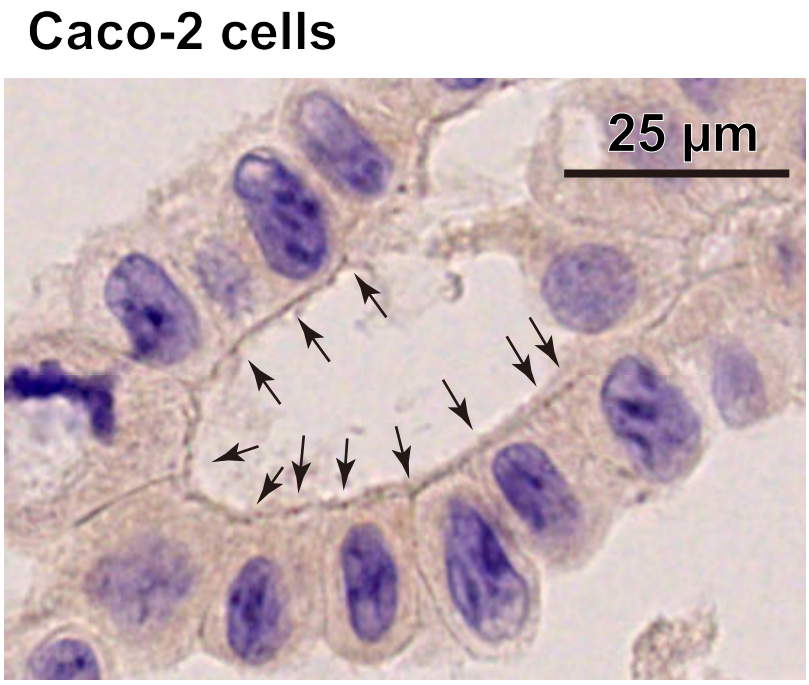

Figure S1. Anti-CLDN15 mAb 2C11 recognizes tight junctions in Caco-2 cells.
Cell sheet of Caco-2 cells were fixed, scraped off from the dish and embedded in the paraffin. The FFPE sample was stained with anti-CLDN15 (2C11). Note that the signal is detected on the cell membranes, especially at the apical tight junctions (arrows).

a

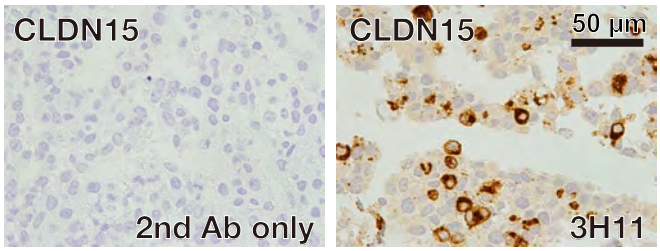

b

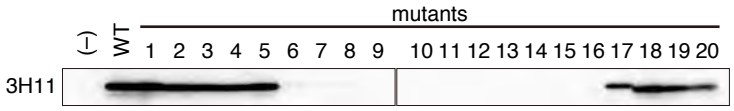

c

Immunoglobulin G2a heavy chain (3H11)

FR1 CDR1 FR2 CDR2 FR3 CDR3 FR4

KLSCAASGFTFSNYVMDWVRQAPKKGLEWVASISTGGGNTYYPDSVKGRFTISRDNAESTLYLQMNSLRSEDTATYYCAASYADYWGQGVMVTVSSAETTAPSV

Immunoglobulin κ light chain (3H11)

FR1 CDR1 FR2 CDR2 FR3 CDR3 FR4

DVVLTQTPPTLSATIGQSVSISCRSSQSLLHSNGNTYLNWLLQRPGQPPQLLIYLVSRLESGVPNRFSGSGSGTDFTLKISGVEAEDLGVYYCVQSTHAPRTFGGGTKLELK

d

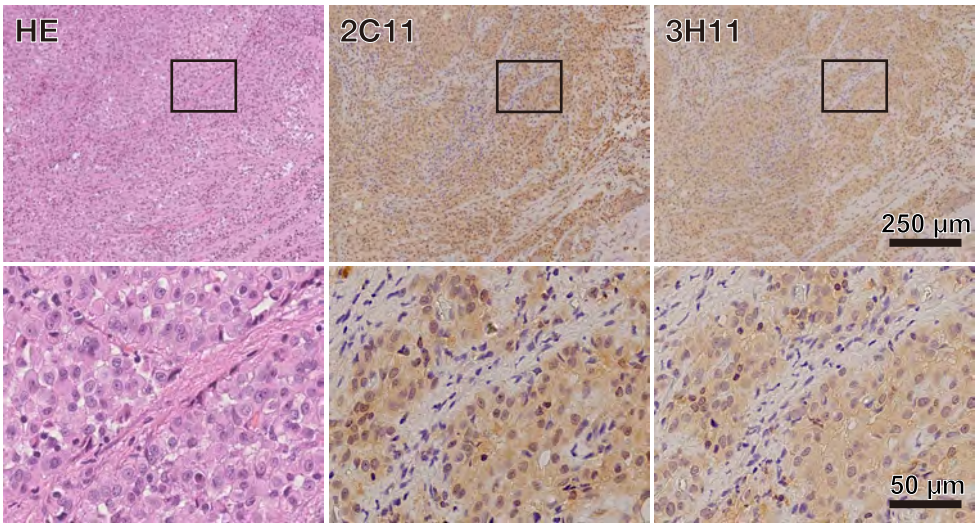

Figure S2. Anti-CLDN15 mAb clones 2C11 and 3H11 exhibit similar staining patterns.

a. IHC of CLDN15-expressing HEK293 cells using anti-CLDN15 (3H11).

b. Epitope analysis of 3H11 using immunoblotting of HEK293T cells expressing CLDN15 mutants shown in Figure 2. Note that 3H11 signal is lost in the mutant 6-16, which corresponds to ^{206}DSSFGKYG^{223} of CLDN15.

c. Amino-acid sequence of the CDRs of 3H11.

d. HE staining and IHC of an epithelioid-type MPM sample using 2C11 and 3H11 mAbs. Note that both clones give similar staining patterns despite their epitopes are different.

Supplementary Table 1. Primers used in the PCR, RT-PCR and real time RT-PCR experiments.

gene	forward	reverse
claudin-1	GAGGTGTCCTACTTTCCTGCTC	TCTCTTCCTTTGCCTCTGTCAC
claudin-2	CCAGGATTCTCGAGCTAAGGAC	CGAGTAGAAGTCCCGAAGGATG
claudin-3	AACTGCGTACAAGACGAGACG	GGTACTAAGGTGAGCAGAGCC
claudin-4	GATGCAGTGCAAGATGTACGAC	CCTACCACTGAGAGAAGCATCC
claudin-5	GTTGGAAATTCTGGGTCTGGTG	ACGATGTTGTGGTCCAGGAAG
claudin-6	TGTTGTCACCCTCCTCATTGTC	AGATGATGCCAGAGATGAGCAC
claudin-7	TCGAGCCTTAATGGTGGTGTC	GGCCTTCTTCGCTTTGTCATC
claudin-8	GGGTTGCCAATTCCATCATCAG	CAGCCTATGTAGAGGGCTTCTC
claudin-9	TAACCCACTGGTTGCGGAAG	GACACGTACAGCAGAGGAGC
claudin-10a	AGATCTCAGCTCTGGTGTGTG	GGTGGTCACTTTCCATTCGTTG
claudin-10b	AAATCGTCGCCTTCGTAGTCTC	TTGGCAAAATAAGTGGCTGTGG
claudin-11	TACGTGCAGGCTTGTAGAGC	GGATGCAGGGGAGAACTGTC
claudin-12	AACTGGCCAAGTGTCTGGTC	AGACCGGCTCAAACTTCCTG
claudin-13	CAAACAAGAGGCCATCAGCTTC	CTGGGTCTGTCTCATCATCTGG
claudin-14	CTAGGCTTCCTGCTTAGCTTCC	ACATTCCATCCACAGTCCCTTC
claudin-15	TGACCCTTTCAAACAGCTACTGG	CAGGTTCTCAAAGATGGTGTTGG
claudin-16	GATCTTCTTCAGTACGCTGCC	TTCACCATCCAACAGTCTGTCC
claudin-17	TCTTCGGTTTGGTTGGGACG	CTGCCGATGAAAGCTGACAC
claudin-18A1	TGTTCCAGTATGAAGGGCTCTG	GCCCAGGATGGTGAAGTATGG
claudin-18A2	TACCAAGGGCTATGGCGTTC	CCCAACAGGGTGAAGTAGCC
claudin-19	GGTCATATCCAGTCAGCACGAG	GTTACTGTCTCCAACCCGAGTG
claudin-20	TTTCCTTTGCTGGAGGAGTCTG	TTTCCGGAATGGTCAGATCCAG
claudin-22	TTAGTCTTCCGAACGGCAACG	CCATGGTCCAGTTCTCCATCTC
claudin-23	GTACTACAGCGACGGACAGC	TCGGGAATCCAACCTTGAGC
claudin-24	CAGCCTCGAGTCACTATGCAG	TACACTTTAGGCTGTACAGTTCCA
occludin	CATATTTGCCTGTGTGGCTTCC	AGGGTAGTTTAGGCTTCCTCCA
tricellulin	ACAGATGACGATCGAGAACGC	TCCAGCTCGTCAAACTTCCTC
marveld3	GGAACAGAGAACGGACCGAG	TCCAAGGCTCTTTGTTCGGATG
rat IgG-HC-RT	5'phos-CCAGGTGCTGGAG	
rat IgG-HC-1st	AACTCTGGAGCCCTGTCCAG	ACTGGCTCAGGGAAATAGCC
rat IgG-HC-2nd	CAGCTGTCCTGCAGTCTGG	GGATAGACAGATGGGGCTGTT
rat IgG-kappa-RT	5'phos-CATGCTGTACGTGC	
rat IgG-kappa-1st	GTGTCAAGTGGAAGATTGATG	CTGATGTCTCTGGGATAGAAG
rat IgG-kappa-2nd	GACAGTGTTACTGATCAGGAC	TACAGTTGGTGCAGCATCAGC

Supplementary methods

Preparation of claudin (CLDN)-expressing cell sample

Expression plasmid vectors encoding a claudin gene (CLDN1, CLDN4, CLDN5, CLDN6, CLDN9, and CLDN15), an internal ribosome entry site (IRES) and a fluorescent protein Venus under the control of the EF1α promoter were prepared. HEK293T cells were transfected with the plasmid using PEI-max (#24765-1; Polysciences, PA, USA). As a negative control, a plasmid vector containing no CLDN gene was used. In addition, 20 plasmids encoding CLDN15 mutants were prepared by PCR in which four amino acids were replaced with alanine or threonine within the immunogen region of the CLND15 gene. The cells were fixed with 10% formalin 48 h after transfection and embedded in paraffin to prepare a paraffin section of a CLDN-expressing cell mass. For immunoblotting, cells were lysed with a sodium dodecyl sulfate (SDS) sample buffer (60 mM Tris-HCl, pH 6.8, 2% SDS, 10% Glycerol, 0.25% Bromophenol blue, 5% 2-mercaptoehanol) 48 h after transfection, and were boiled for 5 min at 95ºC.

Production of rat anti-human CLDN15 mAbs

Monoclonal antibodies against human CLDN15 protein were prepared using the following method according to the rat iliac lymph node method [1]. A peptide corresponding to the 15 amino acids near the carboxy terminus of human CLDN15 (NH_2-Cys-SDQEGDSSFGKYGRNA-COOH) was synthesized (Eurofins Genomics, Tokyo, Japan) and dissolved in PBS to make a 5 mg/ml solution. Then, 2 mg of Imject Maleimide-activated mcKLH (#77606; Thermo Fisher Scientific, MA, USA) was dissolved in 200 µl of distilled water to prepare a 10

mg/ml KLH solution, mixed with the peptide solution, and incubated at RT for 2 h to make a KLH-conjugated peptide antigen. The antigen solution was dialyzed against 150 ml of PBS three times. Next, 250 µl of the antigen solution, 250 µl of PBS and 1 ml of Freund's complete adjuvant (F5881; Sigma-Aldrich, MO, USA) were mixed using two 2 ml Luer lock-type glass syringes and a connector to form an antigen emulsion. An 8-week-old female Wistar rat was anesthetized with isoflurane, and 100 µl of the antigen emulsion was subcutaneously injected into the footpad of each hind limb for immunization. For cell fusion, 5 g of PEG4000 (#109727; Merck millipore, Darmstadt, Germany) was autoclaved and mixed with 8 ml of Dulbecco's Modified Eagle's Medium (DMEM) (D5796; Sigma-Aldrich) and 0.4 ml of dimethyl sulfoxide (D2650; Sigma-Aldrich). Fourteen days after immunization, the rat was euthanized and both iliac lymph nodes were aseptically harvested. The lymph nodes were swollen by injecting a small amount of DMEM and then minced with scissors. The lymph node tissues were crushed and filtered on a 70-µm mesh cell strainer (BD Falcon). The collected lymphocytes were mixed with 1×10^7 SP2 cells, a mouse multiple myeloma-derived cell line, and centrifuged at 1280 rpm for 10 min. After the supernatant was removed and the cell pellet was thoroughly loosened, 1 ml of 50% PEG solution kept at 37ºC was slowly added with gentle mixing over 1 min to fuse the lymphocyte cells and SP2 cells. Two min later, 9 ml of DMEM kept at 37ºC was slowly added dropwise over 5 min to dilute the PEG, and the cells were centrifuged at 900 rpm for 5 min. The supernatant was removed and the cells were resuspended in 40 ml of hybridoma medium (78% GIT medium [#637-25715, Fujifilm WAKO], 2% HAT supplement [#21060017, Thermo Fisher Scientific], 10% BM CondiMed H1 Hybridoma

cloning supplement [#11088947001, Roche, Basel, Switzerland], 10% fetal bovine serum), seeded in four 96-well plates, and cultured at 37ºC in a CO_2 incubator. After 4 to 5 days of seeding, the medium was replaced with 200 µl of fresh hybridoma medium. After two days, hybridoma clones were screened by an enzyme-linked immunosorbent assay (ELISA) using the culture medium and antigen peptide. On the day before ELISA, 100 µl of antigen peptide solution (3 µg/ml in PBS) was added to each well of a 96-well ELISA plate (#655101, Greiner bio-one, Kremsmünster, Austria), and the plate was incubated overnight at 4ºC to coat the surface of the wells with the peptide. PBS alone was used as a negative control. Each well was blocked with a blocking solution (PBS containing 1% BSA) at 37ºC for 1 h, and then incubated with 50 µl of culture supernatant at 37ºC for 1 h. After washing the wells twice with PBS, 50 µl of the secondary antibody solution (horseradish peroxidase [HRP]-linked goat anti-Rat IgG [NA935; GE Healthcare, IL, USA; 1:2000 dilution]) was added to each well and incubated at 37ºC for 1 h. After washing three times with PBS, the plate was developed using 50 µl of 3,3',5,5'-tetramethylbenzidine (TMB) substrate (BioLegend, CA, USA). The reaction was stopped with 50 µl of 1M phosphoric acid, and then the absorbance at 450 nm was quantified. Two clones with a good titer (2C11 and 3H11) were selected.

Sequence analysis of the Complementarity-determining regions (CDRs) of the mAbs

Total RNAs were isolated from the anti-CLDN15 hybridoma clones using TRIzol reagent (#15596026; Thermo Fisher Scientific) according to the manufacturer's

instruction. The variable regions of immunoglobulin heavy and light chains were reverse-transcribed using 5'-Full RACE Core Set (#6122, Takara BIO, Kusatsu, Japan) and primers as shown in Supplementary Table 1. Then, the variable regions were further amplified with nested-PCR using GoTaq DNA polymerase (Promega, WI, USA) or PrimeSTAR GXL DNA Polymerase (Takara BIO) and primers shown in Supplementary Table 1 and cloned into pGEM-T-easy plasmid (#A137A, Promega). The DNA sequence of the plasmid was determined (Macrogen Japan) and the corresponding amino-acid sequences of the CDRs for heavy and light chains were identified.

Immunoblotting

Proteins in the HEK293T cell lysates were separated by SDS-polyacrylamide gel electrophoresis (PAGE) using a 12.5% gel (Fujifilm WAKO), and were transferred onto the PVDF membrane (Immobilon, Merck, Darmstadt, Germany). The membrane was blocked with 5% non-fat dried milk in tris-buffered saline (TBS) containing 0.1% Tween-20 (TBS-T) for 30 min at RT, and incubated with a primary mouse anti-GFP antibody (#598; 1:2000; MBL, Nagoya, Japan) diluted in TBS-T or culture supernatant of hybridomas overnight at 4ºC. After washing with TBS-T, the membrane was incubated with HRP-conjugated anti-Mouse IgG (GE Healthcare; NA931: 1:20000 dilution) or anti-Rat IgG (NA935; 1:5000 dilution) for 1 h at RT. The membrane was then incubated with ECL prime (GE Healthcare) and developed using LAS4000 (GE Healthcare). The gel images were processed using Photoshop (Adobe, CA, USA).

Immunofluorescence microscopy of frozen sections

Tissue sections of 8-μm thickness were fixed with 100% ethanol for 15 min at -20 ºC and washed with PBS three times. After blocking with 2% BSA in PBS, the sections were incubated with rabbit anti-claudin15 polyclonal antibody (pAb) (#18805; IBL, Gumma, Japan) and rat anti-heparan sulfate proteoglycan mAb (HSPG; MAB1948; Merck Millipore) for 30 min at RT. After washing with PBS, the sections were incubated with Alexa Fluor 488-conjugated donkey anti-rabbit IgG pAb (#711-545-150) and Cy3-conjugated donkey anti-rat IgGpAb (#712-165-153), and mounted with Fluoro-Gel II with DAPI (#17985-50, Electron Microscopy Sciences, PA, USA).

RT-PCR

Total RNAs were isolated from the mouse pleura and peritoneum using TRIzol reagent, and cDNA libraries were synthesized using the Primescript II 1st strand cDNA synthesis kit (#6210; Takara BIO). DNA fragments were amplified by PCR with GoTaq DNA polymerase using specific primers for each claudin (listed in Supplementary Table 1). The primer pairs were designed in the same exons, and the DNA fragments amplified from genome served as positive controls. Samples without reverse transcription served as negative controls. The images were recorded using LAS4000 and processed with Photoshop software.

Real-time RT-PCR

Real-time RT-PCR was performed with StepOne Real-Time PCR System (Applied Biosystems, CA, USA). The RT-PCR products were used as templates

for amplification using Thunderbird SYBR qPCR Mix (Toyobo, Osaka, Japan) and specific primers for each claudin (listed in Supplementary Table 1). The relative expression levels were standardized using the DNA fragments amplified from genome DNA, and were normalized to the expression level of *claudin-15*.

1. Kishiro, Y., Kagawa, M., Naito, I. & Sado, Y. A novel method of preparing rat-monoclonal antibody-producing hybridomas by using rat medial iliac lymph node cells. *Cell Struct Funct* **20**, 151-156 (1995).

Original unprocessed gel/blot images

Fig. 1a

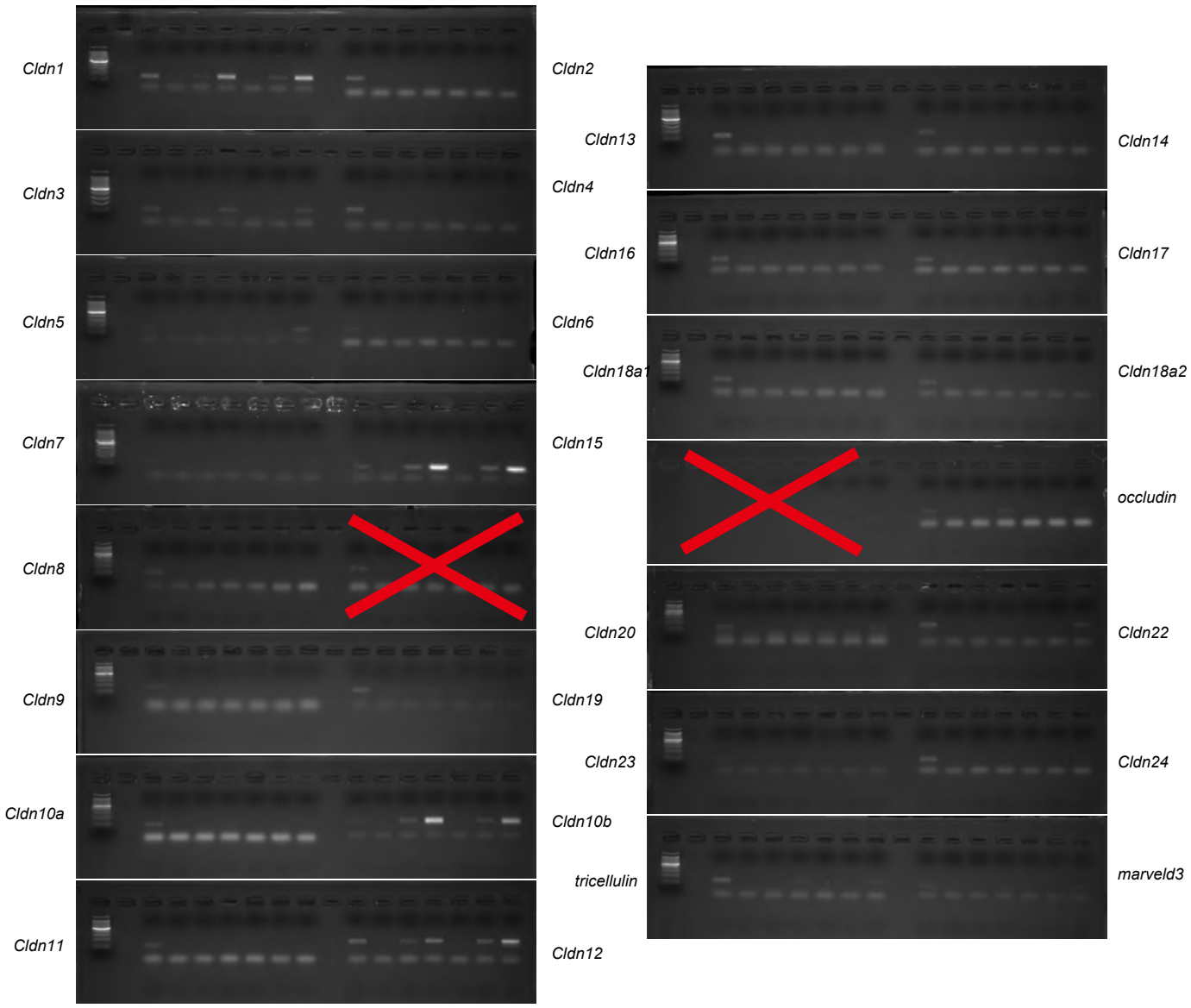

Fig. 2d

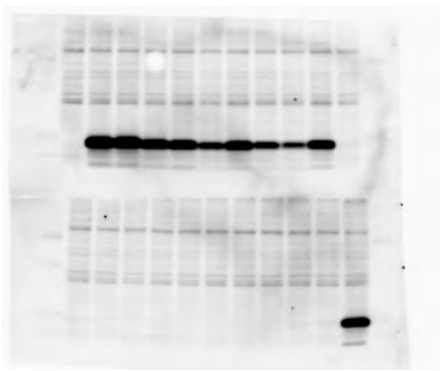

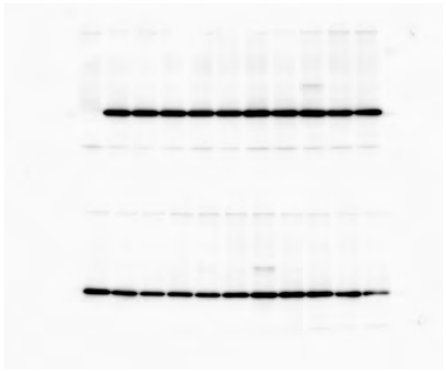

Fig. S2b